

# Oil spill monitoring using satellite imagery in the Sharm El-Maya Bay of Sharm El-Sheikh, Egypt.

M. Morsy<sup>1,2,3, \*</sup>

<sup>1</sup> Institute of Photogrammetry and GeoInformation, Leibniz University Hannover, Nienburger Straße 1, 30167 Hannover, Germany

<sup>2</sup> Geology Department, Faculty of Science, Suez Canal University, Ismailia 41522, Egypt;  
[mona\\_ahmedmorsi@science.suez.edu.eg](mailto:mona_ahmedmorsi@science.suez.edu.eg)

<sup>3</sup> Department Monitoring and Exploration Technologies, Helmholtz Centre for Environmental Research GmbH-UFZ, Permoserstraße 15, 04318 Leipzig, Germany

**KEY WORDS:** Sharm El-Sheikh, Sharm El-Maya, oil spill, pollution, Google Earth Pro, Remote Sensing.

## ABSTRACT:

Sharm el-Sheikh, in Egypt, is a prominent tourist destination. The city attracts millions of visitors annually due to its exceptional location and pleasant climate. Owing to its natural ecosystem and marine diversity, Sharm El-Maya Bay in Sharm el-Sheikh attracts beachgoers and vacationers. In 1999, however, an oil spill occurred at the site. Previous investigations detected a network of buried steel pipelines and a number of buried reinforced concrete tanks, both of which may have contributed to the contamination problem. Although the problem is so detrimental to health and the environment, no follow-up studies were conducted after 2013. Therefore, the author chose to monitor oil leaks over the headland using frequent, high-resolution Google Earth Pro remote sensing data for the years 2017 to 2022. To disclose whether any corrective measures were taken to address the contamination problem. Moreover, to demonstrate if any unanticipated variations have occurred over many years due to climatic factors. The elucidation of the aforementioned issues demonstrates Google Earth Pro's effectiveness in monitoring pollution problems. The results revealed that the area and perimeter of four oil spots had changed slightly over time. During the specified time period, the standard deviations of the four monitored locations fluctuated between 111.1 m<sup>2</sup>, 71.6 m<sup>2</sup>, 83.7 m<sup>2</sup>, and 254.3 m<sup>2</sup>. The research proved that the pollution problem has not improved over time because stakeholders have not reacted. In addition, it highlighted the uniqueness of Google Earth Pro in tracking the changes in oil spot size over a time series.

## 1. INTRODUCTION

When it comes to snorkelling and scuba diving, Sharm el-Sheikh is among the best places in the world. In which the sea is home to many rare and exotic marine life forms and pristine coral reefs. The stakeholders are enticed to move forward with the development and increase the level of luxury with the one-of-a-kind Setting. As a consequence, the city's tourism industry quickly grows, and it draws in millions of visitors annually. Pollution is a major threat to such an environment, and it may be unavoidable due to the beaches' heavy use by tourists and nautical activity. Or because of oil spills from boats and other sources. However, major pollution incidents pose a serious risk to the area, such as the one that occurred in 1999 at Sharm el-Maya Bay of Sharm el-Sheikh and started after the dismantling of the old power plant and its surface fuel storage tanks (Morsy et al., 2010; Khattab et al., 2006; Suez Canal University Report, 2001; Alwany et al., 2007; Carl Bro International Report, 1999; and Cairo University Report, 2001). Its risk threatens the local ecosystem and could reduce the number of tourists who visit each year. The entire headland, the shoreline region, and the water of the sea in the bay are severely impacted by the oil. Morsy et al. (2010) used samples taken from the headland, the shoreline area, and the surrounding water to determine the hydrocarbon concentration. According to the authors, the largest quantities of hydrocarbons were found in samples taken from the headland and the shoreline. The concentration of hydrocarbons was found to be lowest in the water samples. They also assessed the full extent of the oil leak there. Morsy and Rashed (2013) used this research to combine three different non-invasive geophysical techniques (magnetic, gravity, and

ground penetrating radar) to locate the hydrocarbon source there. They discovered three reinforced tanks connected by an underground pipe network beneath the headland. They found that the storage tanks and pipelines had sustained damage, which had caused hydrocarbons to leak. The leakage problem affected the entire bay as well as the extant marine life, but no follow-up studies were published after 2013 regarding the issue.

Consequently, the purpose of this research is to use remote sensing data to track the oil spill over the headland from 2017 to 2022. To reveal the actions that have been taken over the years to clean the site and to determine whether climatic factors play a significant role in reducing the problem over time. However, one of the major controls on the reliability of the data from rather small test sites is high-resolution satellite images. Commonly utilized imagery sources (including Landsat, MODIS, and AVHRR) have a spatial resolution of 30 meters, which makes it difficult to keep an eye on the target problem (Vanderhoof and Burt, 2018). Due to the small size of the study location and the small size of the spots, even better-resolution imagery like Sentinel 2A (10m) and Geoeye-1 (3 m) has limited ability to detect the spill. For free, continuously updated data at a high resolution, we turned to Google Earth Pro>Historical Images (Nagarajan et al., 2022; Taylor et al., 2011 and Warnasuriya et al., 2020). The detection of the oil spills was followed by appropriate statistical metrics to evaluate the changes in the size and extension of oil spots over the years. The proposed concept is based on the research of Morsy et al. (2010), Morsy et al. (2013), and Morsy and Rashed (2013). Because identifying hazardous places over headland with Google Earth Pro imagery is not applicable if no prior

knowledge or field trips have been completed. The proposed idea's innovation is the direct use of Google Earth Pro for the follow-up of the oil spill rather than the use of expensive commercial remote sensing data with high resolution.

## 2. MATERIALS

### 2.1 Study Area

Sharm El-Maya is a bay and headland in the city of Sharm El-Sheikh. The bay is the junction point of the Gulf of Aqaba and the Gulf of Suez, and the shoe-shaped headland separates it from the neighboring Sharm el-Maya bay (Morsy et al., 2010) (Figure 1). The research encompasses the northernmost tip of the headland that overlooks Sharm El-Maya Bay and the entrance to the Red Sea (Morsy et al., 2010; Khattab et al., 2006; and Alwany et al., 2007). The oil spots are detectable by sight and smell because their color is darker than the surrounding soil, their odor is suffocating and heavier than normal fresh air, and their appearance is wetter than the surrounding soil. This facilitates capturing the location of the spots with Google Earth Pro (Figure 2).



**Figure 1.** Location map of Sharm El-Maya Bay area and its surroundings. After Morsy et al. (2013).



**Figure 2.** Shows examples of the oil spots that camera captured. After Morsy et al. (2010).

### 2.2 Google Earth Pro

Google Earth is a virtual globe technology that allows users to explore the environment, track land use/land cover changes (Singhal and Goel, 2021), and contribute and share user-generated data (Yu and Gong, 2012 and Mather et al., 2015). Google Earth is available in three distinct versions, each with its own set of features and pricing structures: Google Earth Free, Google Earth Pro, and Google Earth Enterprise. Business users can subscribe to Google Earth Pro to access enhanced capabilities like GIS and remote sensing (RS) data import, better measurement tools, faster data download speeds, higher resolution printing, and movie making that are not available in the free version of Google Earth (Warnasuriya et al., 2020). Organizations that need to deploy satellite images or significant amounts of geographic data in a secure solution (e.g., run on their own hosting environment on their own servers) can make use of Google Earth Enterprise.

### 2.3 Previous Site Measurements

By using the locations where Morsy et al. (2010) collected soil samples, the tracked oil spot locations in this investigation were double-checked. For their research, the authors collected 47 distinct samples along the headland (Figure 3). Hydrocarbon concentrations varied among the samples that they analyzed. Incorporating sample coordinates into the proposed research gave us confidence in the author's oil spot selections.



**Figure 3.** Shows the 47 collected soil samples. After Morsy et al. (2010).

## 3. METHODS

### 3.1 Imagery Selection

The author selected six Google Earth Pro scenes during the summer, covering the period from 2017 to 2022. As aforementioned, the Google Earth Pro scenes were selected due to their high resolution, which, in our case, increased by several centimeters while zooming in. Moreover, it shows free availability and considerable frequency. The summer time was selected as the hydrocarbons get denser and the color gets darker on the headland (based on the remarks from field trips in 2009 and 2010) (Morsy et al., 2010). Therefore, the selected season positively affected the clarity of the measurements.

### 3.2 Oil Spots Selection

Four oil spots were monitored over time in terms of their area and perimeter. The selection of their locations was based on the

color, width, and length of the contaminated soil. To Avoid overestimating the size of the spill due to the shadow effect, the author ignored the smaller-sized spots and those with lower hydrocarbon concentrations, e.g., lighter-colored spots. The author completed the calculations by tracing each spill with a polygon. Seven years were represented, and a total of 28 polygons were created, as each image has four locations.

### 3.3 Oil Spots Metrics

The area and perimeter of each polygon were measured directly by Google Earth Pro. After the tracing of each oil spot over the whole selected time span from 2017 to 2022. The measures were recorded in an Excel sheet. Excel was used to calculate the increase/decrease in the area and perimeter of each spot over the years. Moreover, the same software was used to calculate the minimum and maximum area and perimeter recorded by each spot over the intended period. Additionally, the mean and standard deviation of each spot were measured for area and perimeter as well.

## 4. RESULTS

### 4.1 Oil Spots Selection

The selection of the oil spots was based on their high contrast with the soil. Their color is almost dark brown to black compared to the neighbouring soil. The first selected spot is located in the north-eastern portion of the study area. Small concrete blocks surround it to the east, and a cliff and the bay's water are to the north. The second spot, on the other hand, occupies the south-western corner of the first one and faces the same Northern cliff and bay. Both the first and second places appear on a single NE-SW inclined line. The third spot faces the first spot's southern corner. It's just next to the concrete fence that limits it from the southern corner. This fence separates the site from east to west. The fourth location is on the western edge of the research site. It's relatively close to the parking lot next to the test location, and its southern corner is facing the concrete fence (Figure 4). Google Earth Pro was efficient in tracking the four spots in all the time-span imagery.



Figure 4. The four selected oil spots.

### 4.2 Oil Spots Verification

The locations of the selected four spots were compared to the locations where the soil samples were collected in 2009 and 2010 (Morsy et al., 2010). The 47 samples appeared to be aligned with the selected spots.

### 4.3 Oil Spots Metrics

In 2018, the total area of spot number one ranged from a minimum of 1080 m<sup>2</sup> to a maximum of 1390 m<sup>2</sup>. In 2019 and 2020, the spot's area was nearly identical, measuring 1313 m<sup>2</sup> and 1311 m<sup>2</sup>, respectively. In contrast, the spot's perimeter ranged from a minimum of 283 m in 2020 to a maximum of 354 m in 2021. The spot's perimeter was comparable in 2018 and 2019 at 308 m and 316 m, respectively. In 2021 and 2022, however, it fluctuated between 354 m and 333 m (Figure 5). The second spot in 2020 and 2021 exhibited very similar areas of 789 m<sup>2</sup> and 801 m<sup>2</sup>. In 2017, 2019, and 2022, the respective measurements for the spot areas were 651 m<sup>2</sup>, 674 m<sup>2</sup>, and 645 m<sup>2</sup>. In 2021, the highest recorded value was 802 m<sup>2</sup>, while the lowest recorded value was 645 m<sup>2</sup> in 2022. In addition, the perimeter ranged from 107 m in 2019 to 134 m in 2018. Figure (6) depicts that in 2017, 2020, 2021, and 2022, the results were 115 m, 119 m, 123 m, and 119 m, respectively. The maximum area recorded at the third spot in 2022 was 1116 m<sup>2</sup>, while the minimum area recorded at the same location in 2017 was 891 m<sup>2</sup>. In 2019 and 2020, the area of the location was very similar (1078 m<sup>2</sup> and 1015 m<sup>2</sup>, respectively). The maximum recorded spot perimeter in 2018 and 2019 was 152 meters for both. While the minimum value recorded in 2020 was 134 million. In 2021 and 2022, the third-place perimeter was nearly identical, measuring 147 m and 146 m respectively (Figure 7). In 2022, the maximum area recorded at the fourth position was 1538 m<sup>2</sup>, while the minimum was 804 m<sup>2</sup> in 2017. Between 2017 and 2022, the perimeter of fourth place fluctuated. The highest recorded value was 279 m in 2022, and the lowest was 231 m in 2017. The measurements showed an upward trend from 2017 to 2022; however, in 2020, there was a deviation of 234 m from the slight incline (Figure 8).

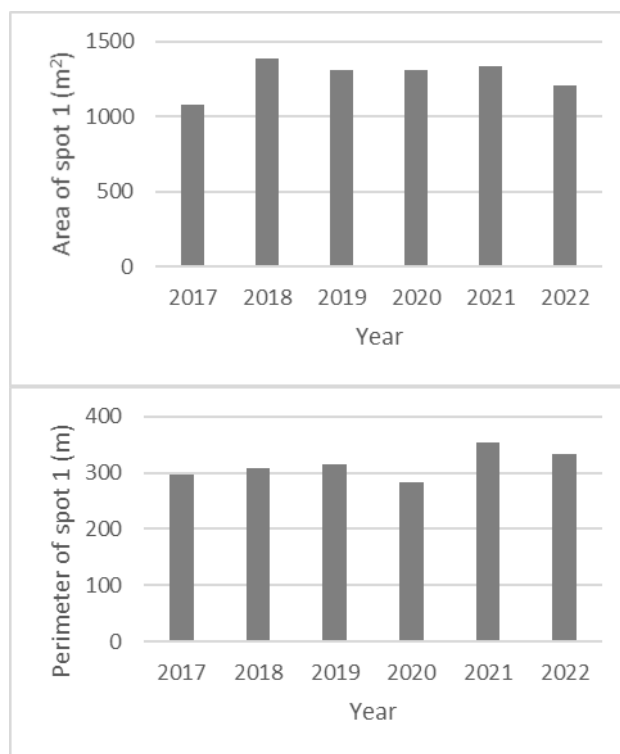
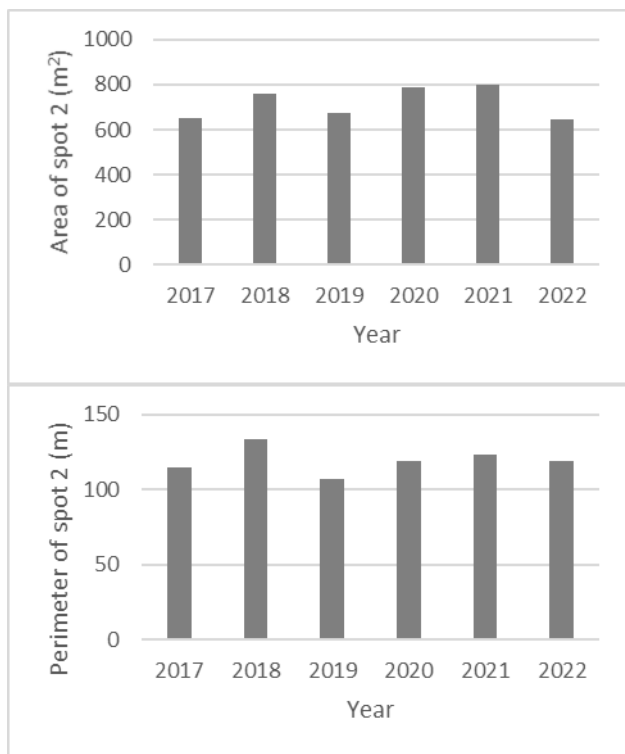
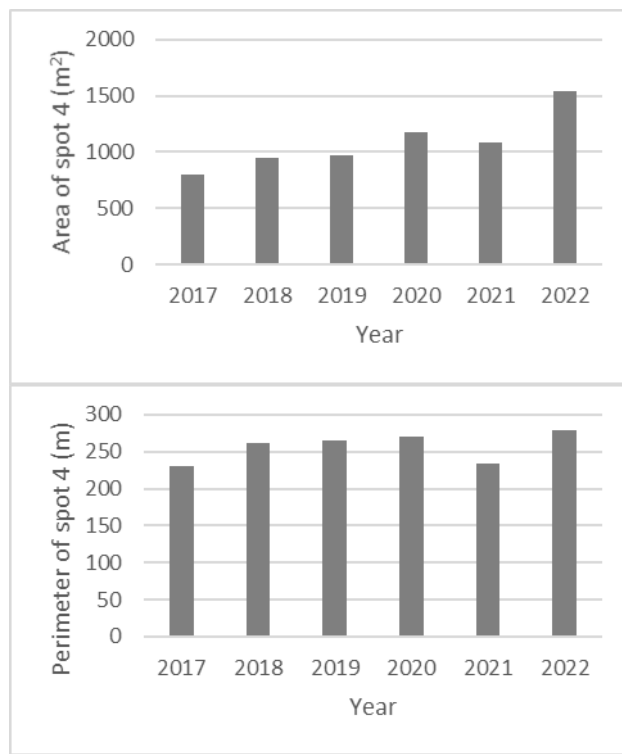


Figure 5. The fluctuation in the area and perimeter of spot No.1 from 2017 to 2022.



**Figure 6.** The fluctuation in the area and perimeter of spot No.2 from 2017 to 2022.



**Figure 8.** The fluctuation in the area and perimeter of spot No.4 from 2017 to 2022.

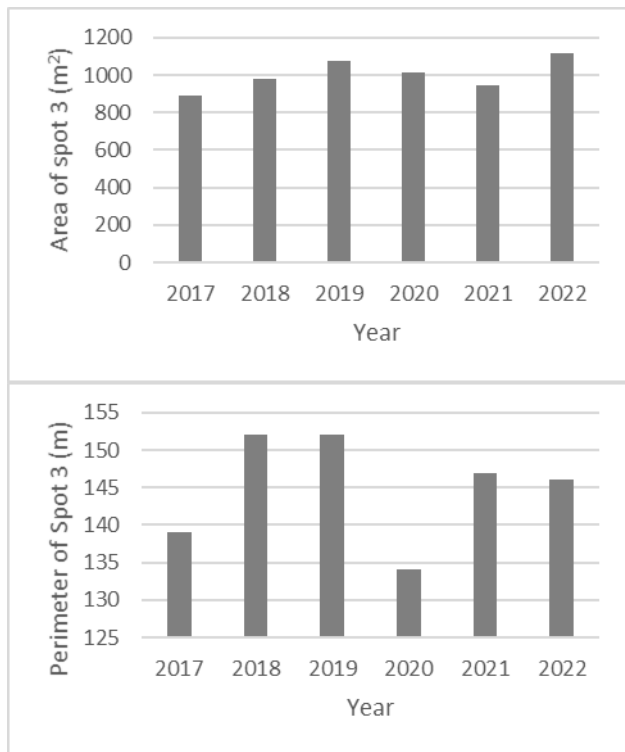


**Figure 7.** The fluctuation in the area and perimeter of spot No.3 from 2017 to 2022.

## 5. DISCUSSION

Sharm El-Maya area is one of the fascinating spots in Sharm-El-Sheikh city, where hundreds of tourists visit the bay annually. The incident of the oil spill, which was a consequence of the dismantling of the old power station that existed over the headland, affected the entire ecosystem of the bay (Morsy et al., 2010). For this reason, studies have been done in order to eliminate the risk of pollution to human health and the ecosystem, e.g., sea life, coral reefs, and marine species. So as a continuation of the studies that have been published between 2010 and 2013, the author tracked four of the existing oil spots using remote sensing data to evaluate the situation at the test site. Data from remote sensing has proven to be supportive of the investigation's goal. Sentinel 2A (10 m) and Geoeye-1 (3 m) were not the optimal choices (Nagarajan et al., 2022), as the study site is limited and required a higher resolution to separate the oil spots. Therefore, the free and available option was Google Earth Pro, which uses Maxar technology and integrates various types of remote sensing data to provide high spatial and temporal resolution and a number of measurement-facilitating options. Figure (9) compares the performance of Geoeye-1 (3 m) commercial imagery with the performance of Google Earth Pro. However, without prior knowledge of the contamination problem, oil spots, and study site in general, it would be impossible for the user to highlight and trace the oil spots using Google Earth Pro.

Each spot's calculated measurements were used to generate descriptive statistics for the four locations. Table (1) displays the minimum and maximum values, the mean, and the standard deviation for each location. Spots 1 and 4 experienced significant alterations over time in their respective size. From 2017 to 2022, the average area of location number one was

1273.8 m<sup>2</sup>, with a standard deviation of 111.1 m<sup>2</sup>. Spot 4 had a mean area of 1089.5 m<sup>2</sup> and a standard deviation of 254.3 m<sup>2</sup>. In 2021, the biggest area was recorded at location No. 1, while in 2022, it was recorded at location No. 4. In contrast, the second and third positions demonstrated less change over the years. The average area of location 2 from 2017 to 2022 was 720.3 m<sup>2</sup>, with a standard deviation of 71.6 m<sup>2</sup>. Table (1) displays that the spot 3 average was 1004.2 m<sup>2</sup> and its standard deviation was 83.7 m<sup>2</sup>. In 2021 and 2022, the biggest areas for spots 2 and 3 were recorded.



**Figure 9.** Compare the performance of Geoeye-1 (3 m) in the upper photo with that of Google Earth Pro in the lower one.

Spot No.	Min area(m <sup>2</sup> )	Max area(m <sup>2</sup> )	Mean(m <sup>2</sup> )	SD(m <sup>2</sup> )
1	1080	1390	1273.8	111.1
2	645	802	720.3	71.6
3	891	1116	1004.2	83.7
4	804	1538	1089.5	254.3

**Table 1.** Shows the minimum (Min) and maximum areas (Max), mean, and standard deviation (SD) of the four spots. The measurements collected by the tracing of the four spots from Google Earth Pro imagery cover the time series between 2017 and 2022.

The perimeter measurements of the spots were compatible with the area measurements. Sites No. 1 and 4 had the greatest standard deviation: 25.4 m and 19.8 m, whereas sites No. 2 and 3 had standard deviations of 3.6 m and 7.2 m, respectively. While the averages for the four locations from 2017 to 2022 are 315.1 m, 119.5 m, 145 m, and 256.8 m (Table 2), respectively,

Spots No. 1 and 4 exhibited the greatest perimeters in 2021 and 2022, whereas spots Nos. 2 and 3 did so in 2018.

Spot No.	Min Perimeter(m)	Max Perimeter(m)	Mean(m)	SD(m)
1	283	354	315.1	25.4
2	107	134	119.5	3.6
3	134	152	145	7.2
4	231	279	256.8	19.8

**Table 2.** Shows the minimum (Min) and maximum perimeter (Max), mean, and standard deviation (SD) of the four spots. The measurements collected by the tracing of the four spots from Google Earth Pro imagery cover the time series between 2017 and 2022.

## 6. CONCLUSION

This study provides insights into the ongoing pollution problem in Sharm el-Maya and a foundation for tracking its progression. Returning to the site of the oil spill on a regular basis to take measurements is an expensive and time-consuming way of monitoring the situation. Remote sensing, on the other hand, is a viable option that can save both time and money while also delivering more regular information on the pollution problem. However, the available high-resolution remote sensing data are insufficient for capturing the small study region and its targeted oil spots, e.g., Sentinel 2A (10 m) and Landsat (30 m). Therefore, commercial data are a possible alternative here, but acquiring the necessary scenes at the required resolution demands a large expenditure of both time and resources. That, after all, may not fit the research requirements, e.g., Geoeye-1 (3 m) (Nagarajan et al., 2022). Google Earth Pro, in this case, provides an innovative option to track the oil spills and provide measurements concerning their size over a considerable time series. It depends on mixing several types of satellite imagery to allow for increasing resolution while zooming in and examining the site from all directions with tilted and vertical moods.

Therefore, the purpose of the current study was to assess any interventions made by the stakeholders, any advancements that have naturally occurred over time as a result of evaporation and high temperatures at the site, and the potential use of Google Earth Pro as a replacement for frequent field trips to the test site. As aforementioned in Section (5) spots No. 1 and 4 showed the highest changes in terms of size, while spots No. 2 and 3 showed lower changes. The maximum recorded sizes were around 2021 and 2022 for all the spots. By following these measurements, we can conclude that no intervention has been made by the stakeholders from 2017 to 2022. Moreover, the situation is exactly the same from 2017 until 2022. Additionally, the measurements clarified that climatic factors (evaporation, temperature, soil moisture, and rainfall) have no effect on the concentration of the hydrocarbon spills because their size and color didn't change drastically after 24 years of the pollution incident. So, there is a pressing need for action to be taken by the stakeholders to clean the headland because the degradation of coral reefs and marine species will never stop if the source of the problem isn't fixed. Moreover, the health of the tourists and swimmers is at risk.

Google Earth Pro is a good substitute for frequent field visits, but it has some limitations. As mentioned in Sections (4 and 5), there are changes in the yearly measurements of each spot. How certain and accurate are the results; This depends on the azimuth and inclination of the used satellites. Add to this the shadow effect in some cases that the author has avoided by capturing the image from different directions. Therefore, a yearly field visit is a must to verify the results of Google Earth Pro. If a couple of field visits prove that the measures are the same, then no more in-situ measures are needed.

Google Earth Pro., however, is sufficient to achieve the target of the presented idea. The clarity and high resolution of the images enabled the vision of all the needed details and the separation of the oil spills with high efficiency. Moreover, prior knowledge of the problem and study site is the key factor in the spot tracking procedure. The use of Google Earth Pro revealed drawbacks, including the very limited available studies dealing with the application. Moreover, downloading the bands of the images is not an option as it comes in RGB. So, there is no chance to classify or find a suitable index to separate the spots with machine learning techniques.

#### ACKNOWLEDGEMENTS

Mona Morsy is supported by Gottfried Wilhelm-Leibniz-Universität Hannover, Institut für Photogrammetrie und GeoInformation, in Hannover and Helmholtz Center for Environmental Research in Leipzig, Germany, UFZ.

I want to express my gratitude to the co-authors and former supervisors who generously supported the first series of publications between 2010 and 2013.

#### REFERENCES

Morsy, M., Soliman, F., Khattab, R., Rashed, M., & El-Masry, N. (2010). Implications of environmental monitoring of oil pollution in Sharm El-Maya Bay, Sharm El-Sheikh, Egypt. *Catrina: The International Journal of Environmental Sciences*, 5(1), 97-103.

Morsy, M. A., Rashed, M. A., El-Masry, N. N., & Soliman, F. A. (2013). Potential Field Methods to Investigate the Source of Hydrocarbon Contamination in Sharm El-Maya Bay Area, Sharm El-Sheikh, Egypt. *Journal of King Abdulaziz University, Earth Sciences*, 24(1), 1-17. doi.org/10.4197/Ear. 24-1.1.

Morsy, M., & Rashed, M. (2013). Integrated magnetic, gravity, and GPR surveys to locate the probable source of hydrocarbon contamination in Sharm El-Sheikh area, south Sinai, Egypt. *Journal of Applied Geophysics*, 88, 131-138. <https://doi.org/10.1016/j.jappgeo.2012.11.003>.

Alwany, M., Hanafy, M., Kotb, M., & Gab-Alla, A. (2007). Species Diversity and Habitat Distribution of Fishes in Sharm El-Maiya Bay, Sharm El-Sheikh, Red Sea. *Catrina: The International Journal of Environmental Sciences*, 2(1), 83-90.

Cairo University. (2001). Cleaning up Sharm El-Maya, Sharm El-Sheikh, southern Sinai, from the petroleum materials (Final Report). *Center for Environmental Hazards Mitigation*, Giza, Egypt.

Carl Bro International a/s. (1999). Mitigation Measures for Environmental Problems in Sharm El- Maya Bay, Sharm El-Sheikh, Egypt (Final Report).

Khattab, R., Temraz, T., Kotb, M., & Hanafy, M. (2006). Assessment of Oil Pollution Situation in Sharm El-Maiya Bay, Sharm El-Sheikh South Sinai, Egypt. *Catrina: The International Journal of Environmental Sciences*, 1(1), 33-40.

Suez Canal University. (2001). Environmental Monitoring Program for Sharm El-Maya Bay (Final Report). *Faculty of Science, Marine Biology Department, Ismailia, Egypt*.

Vanderhoof MK, Burt C. Applying High-Resolution Imagery to Evaluate Restoration-Induced Changes in Stream Condition, Missouri River Headwaters Basin, Montana. *Remote Sensing*. 2018; 10(6):913. doi.org/10.3390/rs10060913.

Yu, L., & Gong, P. (2012). Google Earth as a virtual globe tool for Earth science applications at the global scale: progress and perspectives. *International Journal of Remote Sensing*, 33(12), 3966-3986. doi.org/10.1080/01431161.2011.636081.

Taylor, B. T., Fernando, P., Bauman, A. E., Williamson, A., Craig, J. C., & Redman, S. (2011). Measuring the quality of public open space using Google Earth. *American journal of preventive medicine*, 40(2), 105-112. doi.org/10.1016/j.amepre.2010.10.024.

Warnasuriya, T. W. S., Kumara, M. P., Gunasekara, S. S., Gunaalan, K., & Jayathilaka, R. M. R. M. (2020). An improved method to detect shoreline changes in small-scale beaches using Google Earth Pro. *Marine Geodesy*, 43(6), 541-572. doi.org/10.1080/01490419.2020.1822478

Mather, A. E., Mills, S., Stokes, M., & Fyfe, R. (2015). Ten years on: what can Google Earth offer the geoscience community? *Geology Today*, 31(6), 216-221. doi.org/10.1111/gto.12119

Singhal, A., & Goel, S. (2021). Spatio-temporal analysis of open waste dumping sites using google earth: A case study of Kharagpur City, India. *Spatial Modeling and Assessment of Environmental Contaminants: Risk Assessment and Remediation*, 137-151. doi.org/10.1007/978-3-030-63422-3\_9.

Nagarajan, P., Rajendran, L., Pillai, N. D., & Lakshmanan, G. (2022). Comparison of machine learning algorithms for mangrove species identification in Malad creek, Mumbai using WorldView-2 and Google Earth images. *Journal of Coastal Conservation*, 26(5), 44. doi.org/10.1007/s11852-022-00891-2.